

---

This is an electronic reprint of the original article.  
This reprint may differ from the original in pagination and typographic detail.

Baidya, Avijit; Yatheendran, Anagha; Ahuja, Tripti; Sudhakar, Chennu; Das, Sarit Kumar; Ras, Robin H.A.; Pradeep, Thalappil

## Waterborne Fluorine-Free Superhydrophobic Surfaces Exhibiting Simultaneous CO<sub>2</sub> and Humidity Sorption

*Published in:*  
Advanced Materials Interfaces

*DOI:*  
[10.1002/admi.201901013](https://doi.org/10.1002/admi.201901013)

Published: 01/01/2019

*Document Version*  
Peer reviewed version

*Published under the following license:*  
CC BY-NC

*Please cite the original version:*  
Baidya, A., Yatheendran, A., Ahuja, T., Sudhakar, C., Das, S. K., Ras, R. H. A., & Pradeep, T. (2019). Waterborne Fluorine-Free Superhydrophobic Surfaces Exhibiting Simultaneous CO<sub>2</sub> and Humidity Sorption. *Advanced Materials Interfaces*, 1-8. [1901013]. <https://doi.org/10.1002/admi.201901013>

---

This material is protected by copyright and other intellectual property rights, and duplication or sale of all or part of any of the repository collections is not permitted, except that material may be duplicated by you for your research use or educational purposes in electronic or print form. You must obtain permission for any other use. Electronic or print copies may not be offered, whether for sale or otherwise to anyone who is not an authorised user.

DOI: 10.1002/ ((please add manuscript number))

Article type: (Article)

## Waterborne Fluorine-Free Superhydrophobic Surfaces Exhibiting Simultaneous CO<sub>2</sub> and Humidity Sorption

*Avijit Baidya<sup>a,b,c</sup>, Anagha Yatheendran<sup>a</sup>, Tripti Ahuja<sup>a</sup>, Chennu Sudhakar<sup>a</sup>, Sarit Kumar Das<sup>c</sup>, Robin H.A. Ras<sup>b,d</sup>, Thalappil Pradeep<sup>a,\*</sup>*

Dr. Avijit Baidya, Anagha Yatheendran, Tripti Ahuja, Chennu Sudhakar, Prof. Thalappil Pradeep

<sup>a</sup>DST Unit of Nanoscience, Thematic Unit of Excellence, Department of Chemistry, Indian Institute of Technology Madras, Chennai, India

E-mail: [pradeep@iitm.ac.in](mailto:pradeep@iitm.ac.in)

Dr. Avijit Baidya, Prof. Robin H.A. Ras

<sup>b</sup>Department of Applied Physics, Aalto University School of Science, Puumiehenkuja 2, 02150 Espoo, Finland

Dr. Avijit Baidya, Prof. Sarit Kumar Das

<sup>c</sup>Department of Mechanical Engineering, Indian Institute of Technology Madras, Chennai 600036, India

Prof. Robin H.A. Ras

<sup>d</sup>Department of Bioproducts and Biosystems, Aalto University School of Chemical Engineering, Kemistintie 1, 02150 Espoo, Finland

Keywords: superhydrophobicity, environment-friendly, waterborne, robust, moisture sorption and CO<sub>2</sub> capture

Recent progress in the field of superhydrophobic materials has proven their potential to solve many problems of the contemporary society. However, the use of such materials to capture moisture and CO<sub>2</sub> from air, to help reduce the impact of global climate change has not been explored. In addition, most of the time, fabrication of these materials needs organic solvents and fluorinated molecules involving multiple steps that hinder the use of non-wettable materials in everyday life. Herein, we report a waterborne, fluorine-free, robust superhydrophobic material synthesized at room temperature through a one-step chemical-modification process, which exhibits moisture and CO<sub>2</sub> capturing capability. While covalently-grafted low surface energy hydrocarbon molecules control the bulk superhydrophobicity, the incorporated amine

functionalities facilitate moisture and CO<sub>2</sub> adsorption as these molecules (H<sub>2</sub>O and CO<sub>2</sub>) can easily diffuse through hydrocarbon assemblies. Being polar, H<sub>2</sub>O molecules were observed to readily interact with amine groups and favor the adsorption process. Synthesized material shows an approximate CO<sub>2</sub> adsorption of 480 ppm (10.90 mmol/L) in ambient conditions having 75% humidity. Multi-functionality along with durability of this material will help expand the applications of superhydrophobic materials.

## 1. Introduction

Mimicking natural phenomena is probably the best way to explore smartness. Over the years this has made Mother Nature an idol of architecture. Among many others, surfaces of various biological species having interesting non-wetting characteristics have attracted both industry and academia, and have become some of the intensely pursued research areas because of their enormous potential in various domains.<sup>[1]</sup> Although several methodologies have been introduced to fabricate these surfaces, complicated multi-step processes, limitation in large area production, durability, *etc.*, have restricted their use in everyday life.<sup>[2]</sup> Recently, a few such robust liquid repelling surfaces have been reported.<sup>[2c, 3]</sup> However, in most of the cases, achieving such a property involves the use of (1) fluorine-containing chemicals (offering low surface energy) and (2) hazardous organic solvents.<sup>[3a, 4]</sup> While fluorinated hydrocarbons can lead to bioaccumulation and toxicity, the use of organic solvents increases environmental concerns.<sup>[5]</sup> Recently, a few superhydrophobic materials have also been designed with reduced environmental impact.<sup>[6]</sup> For example, Chen *et al.* have demonstrated the fabrication of a fluorine-free robust superhydrophobic surface, but organic solvents were used in the process.<sup>[7]</sup> We have shown the fabrication of organic-solvent-free superhydrophobic materials that contain fluorinated molecules.<sup>[8]</sup> Therefore, designing a water-based fluorine-free robust low energy materials at ambient conditions is important from the perspective of reduced environmental impact and industrial significance.

Imparting new properties such as conductivity, chemical sensitivity, *etc.*, especially to non-wettable materials is important.<sup>[9]</sup> For example, introduction of carbon-based materials like graphite, reduced-graphene, and carbon nanotubes to enhance the mechanical, thermal and electrical conductivity,<sup>[10]</sup> incorporation of inorganic nanoparticles like TiO<sub>2</sub>, and ZnO to impart bio-degradation, *etc.*,<sup>[2a, 11]</sup> to superhydrophobic surfaces are well-known. However, in most of the cases, these modified surfaces were developed through the incorporation of different micro/nanomaterials. In contrast, fabrication of superhydrophobic materials having molecularly-grafted functionalities to address various environmentally-relevant problems have not been explored. In the context of recent concerns about the climate change, both moisture and CO<sub>2</sub> have great influence on the rise of atmospheric temperature. Although some superhydrophobic/omniphobic membranes<sup>[12]</sup> and MOFs (metal organic frameworks)<sup>[13]</sup> are known to capture CO<sub>2</sub>, their fabrication processes involve multiple steps, hazardous organic solvents and fluorine-containing molecules. In the case of membranes, liquid repelling property enhances gas diffusion through them as the pores are not blocked by water molecules. CO<sub>2</sub> diffusion through the membranes are typically dissolved and separated by alkaline amine solutions.<sup>[12a]</sup> For MOFs, even though it shows an uptake of approximately 11.0 mol/L at 298 K and 55 bar with 100 mg of the material, stability, complex fabrication protocols, bio and environmental-compatibility as well as industrial scale production require additional efforts. These limit the usability of these materials in everyday life even though they may possess good CO<sub>2</sub> adsorption capability.

Herein, we have designed an environment-friendly waterborne clay-based material at ambient conditions that provides a robust large-area superhydrophobic coating at room temperature and adsorbs moisture (water vapor) and CO<sub>2</sub> from air at the same time without affecting its non-wetting property. These multifunctional properties of the material arise from the covalently-grafted chemical-functionalities having different molecular dimensions. While the incorporated hydrocarbon chain decreases the surface free energy of the material, amino functionalities

(wrapped with clay sheets) facilitate adsorption of moisture and CO<sub>2</sub> through electronegative nitrogen atoms. Being synthesized and dispersed in water at neutral pH, it also minimizes the safety concerns, environmental pollution and operational cost, enhancing industrial viability. Applicability of this material to develop a robust and flexible waterproof paper is also demonstrated and tested with various external perturbations. In short, herein a waterborne green superhydrophobic material is developed through a one-step wet-chemical process that possesses environmentally-relevant multifunctional properties and shows potential applicability in various industries like paints, packaging, clothing, paper, *etc.*

## 2. Results and Discussion

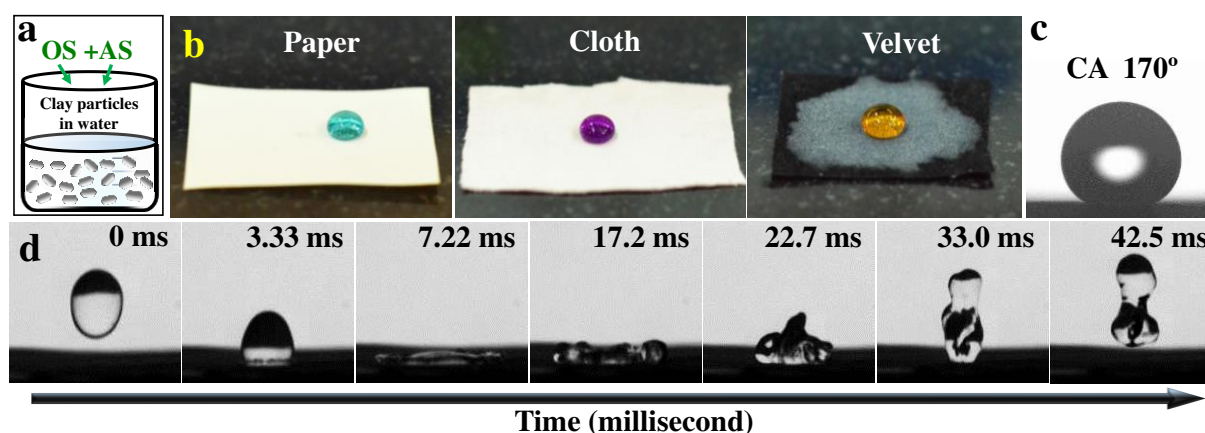


**Figure 1.** a, Schematic representation of the synthesis of a waterborne superhydrophobic material. b, Photograph of colored water droplets over various coated substrates. Aqueous solutions of CuCl<sub>2</sub>, KMnO<sub>4</sub> and K<sub>2</sub>Cr<sub>2</sub>O<sub>7</sub> were used instead of pure water to add color contrast. c, Static water contact angle over a superhydrophobic paper. d, Time resolved bouncing of water droplet over a coated filter paper (soft surface).

**Figure 1a** schematically represents one-pot chemical modification of native clay (NC) particles with two different types of silanes, octadecyltriethoxysilane (OS) and 3-(2-aminoethylamino)propyltrimethoxysilane (AS), at room temperature, in water. This results in

excellent water-repelling thin films upon spray coating the suspension over various soft and hard substrates (Figure 1b). OS molecules, that possess low surface energy because of the hydrocarbon chain, get slowly adsorbed over clay sheets through hydroxyl groups and finally form covalent bonds through hydrolysis.<sup>[8a]</sup> These hydrocarbon chains introduce non-wetting characteristics to the hydrophilic clay material that forced water droplet to sit as a sphere having a static contact angle (CA) of 170° (Figure 1c). Thermodynamically, it also minimizes the air-water-solid interfacial energy of water droplet and facilitates its rolling-off. Water-repelling property of the material was evaluated with advancing and receding contact angle (AC and RC) and contact angle hysteresis (CAH) measurements, which are more sensitive to the droplet dynamics on the surface (Figure S1). This was further extended to droplet drag test (DDT) and vertical droplet adhesion test (VDAT)<sup>[8a]</sup> (Figure S2 & Video V1,V2) (experimental section). Bouncing of a water droplet even over a soft surface (coated filter paper) is pictorially presented in Figure 1d & Video V3.

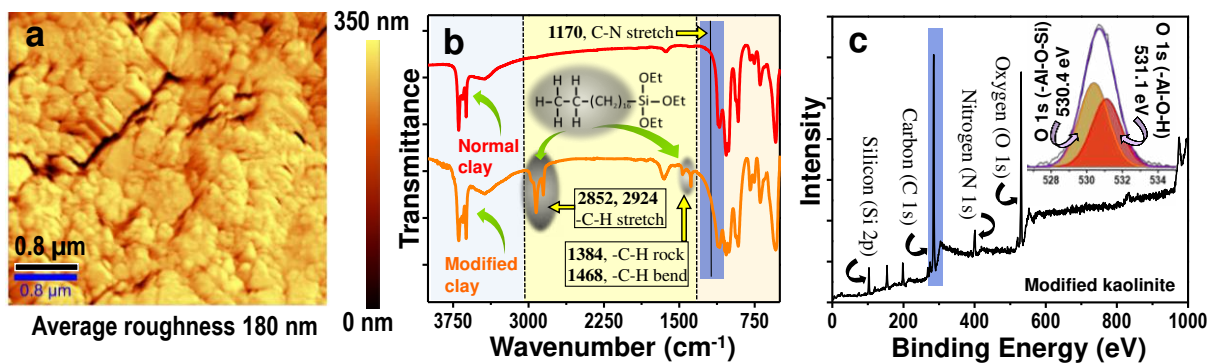


**Figure 2.** a, AFM image of the coated glass substrate reveals the roughness of the coating (average roughness 180 nm.). b, IR spectra of the superhydrophobic material (normal and modified clay). Peaks at 2852, 2924 1384, and 1468  $\text{cm}^{-1}$  (marked area) correspond to various vibrational modes of the C-H bond. Shoulder at 1170  $\text{cm}^{-1}$  (for expanded view, see Figure S6), which broadened the spectrum, corresponds to C-N stretching. c, Survey and deconvoluted XPS spectra in the O1s region showing the relative concentrations of Al-O-H and Al-O-Si linkages, over chemically functionalized clay-coated surface.

Modified clay (MC) induces nanoscale surface roughness, one of the pre-requirements for superhydrophobicity, which was revealed through atomic force microscopy (AFM) (**Figure 2a**).

While average surface roughness of the coated glass surface was ~180 nm, NC coated glass surface showed an average roughness of 30 nm (Figure S3). Such enhancement in roughness is known to be controlled by the hydrophobic effect,<sup>[8a]</sup> namely an interaction between water and low surface energy molecules. Surface morphology of MC coated filter paper was imaged by scanning electron microscopy (SEM) with a tilt angle of 45° (Figure S4). Uniformly distributed nanoscale features over micron sized fibrous matrices facilitate the trapping of air, leading to an excellent water-repelling property. Inset demonstrates the top/perpendicular view (0°) of the surface. Figure S5 demonstrates the cross-sectional view of the layered superhydrophobic thin film, coated over a glass substrate. Average thickness of the coating was 8-10 μm.

Mode of attachment of the incorporated chemical-functionalities with NC particles, being the underlying reason to provide durable superhydrophobicity, was studied with infrared spectroscopy (IR) and X-ray photoelectron spectroscopy (XPS). Additional peaks at 2852, 2924, 1384, and 1468 cm<sup>-1</sup> (marked) in the IR spectrum of MC particles are related to the stretching, rocking and bending vibrational modes of the C-H bond (Figure 2b). This confirmed the chemical attachment of AS and OS with NC particles which is solely inorganic in nature (being an aluminosilicate). Apart from this, a shoulder at 1170 cm<sup>-1</sup> (marked, expanded view Figure S6), which is associated with the broadening of IR spectrum of MC in the region of 1100 to 1200 cm<sup>-1</sup>, is related to the C-N stretching. NC particles (kaolinite) mostly consist of Al-O-H and Al-O-Si groups where the upper-most layer of the surface contains relatively higher concentration of Al-O-H (than Al-O-Si) groups (Figure S7). These active O-H groups readily react with silane molecules resulting in an increase of Al-O-Si network over the surface. Figure 2c shows the relative concentrations of Al-O-H and Al-O-Si for the MC coated surface. Incorporation of hydrocarbon functionalities over the clay surfaces also reflects the presence of substantial amount of carbon (Figure 2c) compared to the unmodified one (Figure S8). Small

peak in the region of 285 eV in the spectrum of the NC corresponds to carbon, which mostly comes from the organic species (Figure S8). Eventually, the covalent attachment between Si (from OS or AS) and OH (from NC) leads to the long-standing stability of the material. This was also tested by keeping both the as-synthesized MC dispersion and the coated substrates for 3 months at normal atmospheric condition and room temperature (30-38 °C) (experimental section) in the laboratory condition.

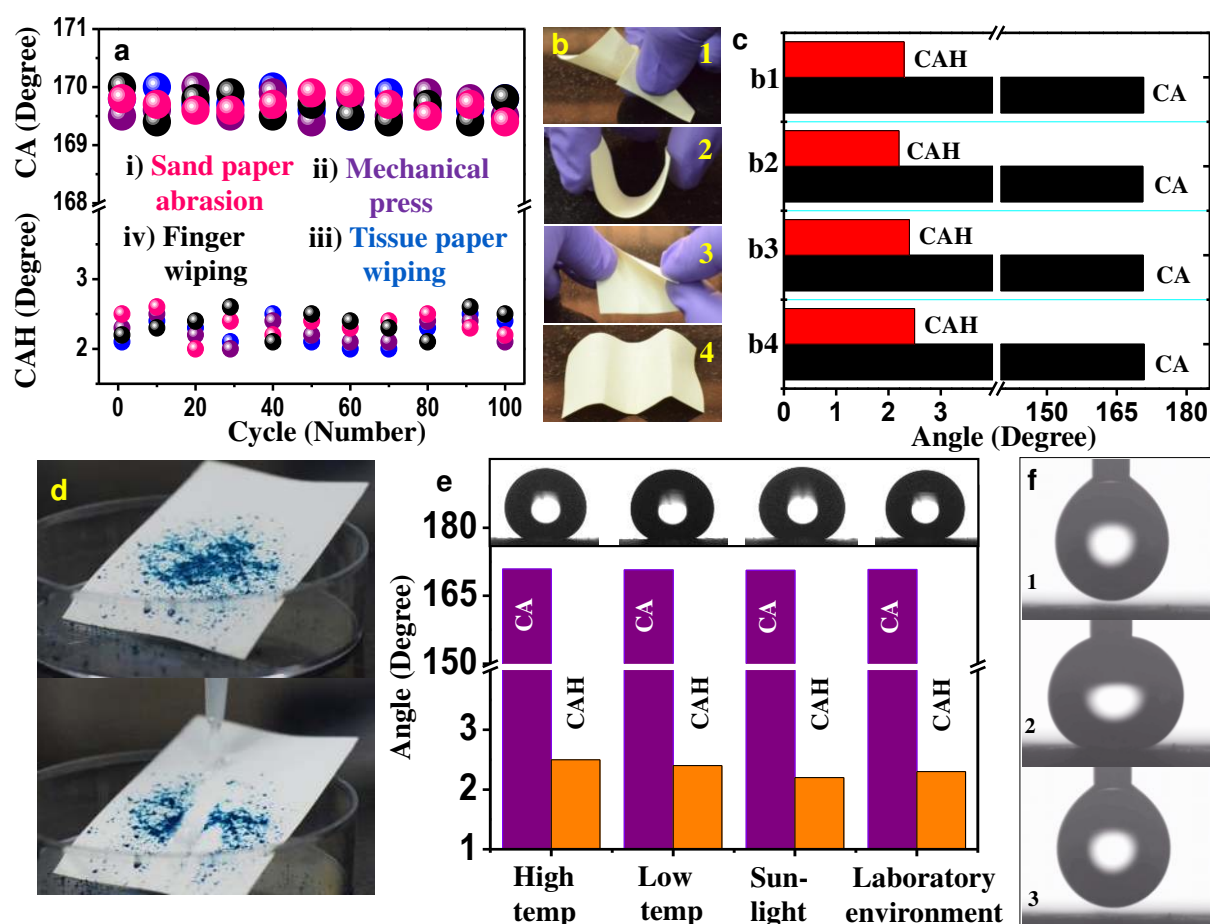


**Figure 3.** a, Durability of the water-repelling surface in terms of the change in CA and CAH of water droplet during multiple abrasion cycles. (i) Sand paper abrasion with 50 g of load (abrasion distance of 5 cm), (ii) mechanical pressing with a pressure of 264.4 atm (equivalent to the weight of 5 ton), (iii) tissue paper abrasion and (iv) finger wiping test. b, Possible bending movements of the superhydrophobic paper (1-4). c, Change of non-wetting property of the superhydrophobic paper (presented through static CA and CAH) upon manual bending cycles



illustrated in (b), for 100 times. d, Water-repelling and self-cleaning property of the coated paper after treating with an organic solvent (THF treated surface is demonstrated here). Water droplets carry the dust and roll off. e, Durability of the coated paper upon various environmental perturbations such as temperature treatments for 2 h (150 and -80 °C), exposure to direct sunlight and normal laboratory environment for 3 months. Inset, static contact angles of water droplet after corresponding experiments. f, Vertical droplet adhesion test over high-temp-treated superhydrophobic surface (1-3). Detachment of the water droplet without leaving any trace of water over the treated surface proves the retained non-wetting property of the coated substrate.

Mechanical durability being an essential parameter towards various industrial applications, MC coated superhydrophobic surfaces were tested with several hard and soft abrasion tests. Static and dynamic contact angles of water droplets over abraded surfaces are graphically presented in **Figure 3a**. After every 10 completed abrasion cycles, water CA were measured and continued for 100 cycles. For instance, in the hard abrasion tests, the coated surface was subjected to sand paper abrasion test with a load of 50 g and mechanical-pressing test with a pressure of 264.4 atm (equivalent to a weight of 5 ton) (Figure S9 i&ii). In the first case, even though 100 abrasion cycles result in the removal of a few layers of the coating, the underlying layers helped to retain their water-repelling property intact<sup>[8a, 14]</sup> and made water droplets to roll-off through the abraded surface areas (Figure 3a). Similar water-repellent property was observed after mechanical-pressing test where the coated surface was subjected to a pressure of 264.4 atm (equivalent to a weight of 5 ton) (Figure S9ii, see experimental section for details). For soft abrasions, the coated surface was tested with tissue paper abrasion and finger wiping test in a cyclic fashion (Figure S9iii&iv). Here also, non-wettability was unchanged with spontaneous rolling-off of the water droplets through the abraded areas (Figure 3a). Unaltered superhydrophobicity of the abraded surface was further examined with DDT and VDAT. DDT

over finger-wiped surface and VDAT over sand paper abraded surface are presented in Figure S10a&b and Video V4, V5. To demonstrate the applicability of the material for various paper-based technologies, the coated superhydrophobic paper was subjected to various manual-bending-movements (Figure 3b, 1-4) that are comparable to everyday applications. These were performed 100 times and the treated-surfaces were evaluated with CA and CAH measurements (Figure 3c). Durability of the coated surface was further tested with the oil-wash experiment (Figure S11, experimental section) where the superhydrophobic surface (filter paper) was artificially wetted with silicone oil and washed manually with ethanol and hexane. Retention of water-repelling characteristic upon the above-mentioned experiments not only proves the durability of the material, it also showed the effective binding of the material with the substrate without any adhesive. This binding is due to the self-polymerization of secondary amine groups during the spontaneous drying process<sup>[8a]</sup> that assists the binding between the clay particles as well as between the material and the substrate. These bending experiments also demonstrate the flexibility of the coated paper.

Similar to the mechanical durability, stability of the material towards low-surface-tension liquids that stick and penetrate the surface easily, was tested with multiple organic solvents having a range of polarity (experimental section). In the first case, surfaces were washed with different organic solvents and tested with the movement of water droplets after proper drying. In all the cases, surfaces were observed to maintain their superhydrophobicity and self-cleaning property. This is presented for THF-treated surface in Figure 3d (pictorially) and Video V6. In the second case, surfaces were immersed in selected solvents and kept for a long time (50 h) at room temperature in a closed container (to avoid the evaporation of the solvents). Water-repelling property of these surfaces was evaluated through CA and CAH measurements after every 5 h interval (Figure S12). Behavior of acidic and basic (pH=1 & pH=14) water droplets over the coated surface was tested with CA measurements and VDATs (Figure S13 & S14). Effect of various extreme environmental conditions such as high-temp (150 °C), low-temp (-

80 °C), exposure to direct sunlight and normal laboratory conditions for long time were also tested in order to test the industrial relevance of this material (Figure 3e). Details are given in the experimental section. Inset shows the CA of the water droplet after corresponding experiment. Treated surfaces were further tested with VDAT. Figure 3f and Video V7 correspond to VDAT over high-temp-treated surfaces. Temperature stability of the material was further investigated in detail till 250 °C and the exposed surfaces were studied with CA and VDAT measurements (Figure S15a & b, experimental section). VDAT with 250 °C temperature treated surface was presented in Figure S15b.

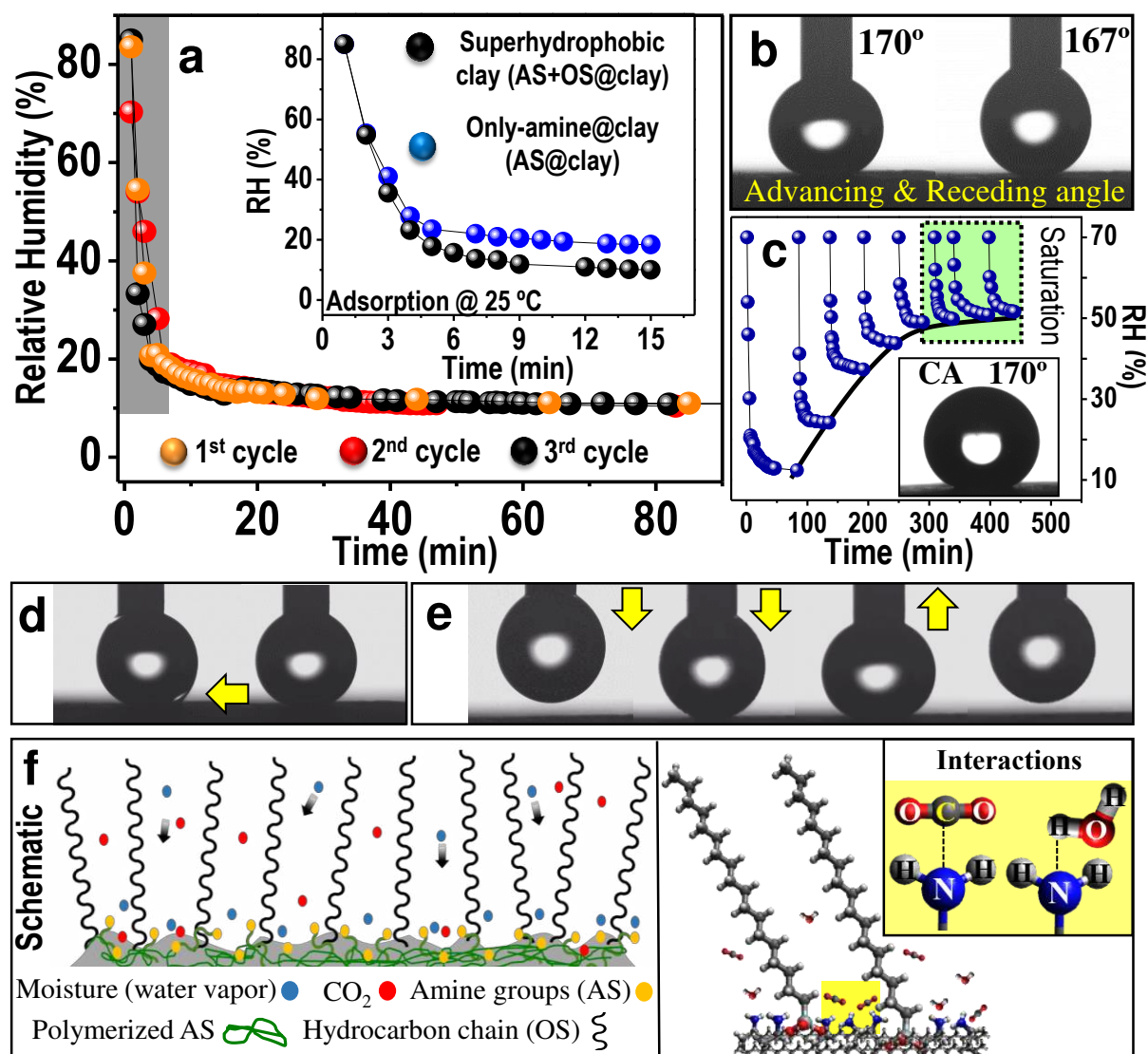


**Figure 4.** a, Rapid adsorption of moisture by superhydrophobic material at constant temperature. (Inset) Experiments with amine functionalized (AS@clay) and superhydrophobic (AS+OS@clay) surfaces prove that the amine functionalities are the underlying reason for moisture adsorption. Control experiment with NC is shown in Figure S16. Both amine-functionalized clay and superhydrophobic clay contain the same amount of amine functionality. b, Advancing and receding water contact angles over superhydrophobic surface after the moisture-adsorption experiment (a). c, Consecutive cycles to achieve moisture saturation of the coated surface at constant temperature. Black curve represents the sigmoidal nature of moisture adsorption towards saturation. (Inset) Static CA of water droplet over saturated superhydrophobic surface derived from the experiment (c). Droplet drag test (d) and vertical droplet adhesion test (e) over moisture saturated superhydrophobic surface. f, A molecular-surface-functionality model to illustrate the moisture adsorption phenomenon over functional superhydrophobic material. Assembled hydrocarbon chains that control the bulk non-wettability (by decreasing surface energy and trapped air) but allow air molecules (moisture and CO<sub>2</sub>) to diffuse into the assemblies. Inset, interactions between electronegative nitrogen atom of amine group with water and CO<sub>2</sub>.

Apart from superhydrophobicity, the synthesized material showed interesting and environmentally-relevant properties, such as adsorption of moisture and CO<sub>2</sub>. To demonstrate the moisture capturing ability of the material, coated filter papers were subjected to humid air (85% relative humidity, RH) in a closed container and change of RH with time was studied at constant temperature (25 °C). Surprisingly, within two minutes, RH of the enclosure was seen to decrease to less than 20% (marked, **Figure 4a**) and finally reached a constant value of 10±2% RH with time. This change in RH was not seen for filter paper and NC (Figure S16). Amino-functionalities being the active sites to facilitate moisture-adsorption, along with the superhydrophobic material (AS+OS@clay) that contain AS, a control study was performed

with only-amine functionalized clay (AS@clay) (Figure 4a, inset). Similar decrease of RH for both the cases revealed the moisture-adsorption mechanism as well as the importance of amino-functionalities to impart such a property to the coating material. Being an electronegative element, nitrogen atoms easily interact with water molecules through hydrogen bonds and facilitate adsorption of water. It is also possible through the electrostatic interaction between amine and water molecules, as secondary amine groups sometimes possess distinct positive charges. This reflects the fast adsorption kinetics of water molecules. Comparatively less adsorption of moisture for AS@clay compared to the AS+OS@clay, although concentration of amine-functionality was equal in both the materials, suggests that along with the presence of active-chemical-functionalities, hydrophobic effect-induced enhancement of surface roughness (Figure 2a) results in higher surface exposure for the AS+OS@clay. However, the kinetics of this moisture-adsorption was seen to be identical for both the materials, at constant temperature (25 °C). As surrounding temperature having a great influence on both RH and adsorption kinetics, temperature-dependent studies were performed with constant initial RH of 85% (Figure S17) where negligible difference in the moisture adsorption was observed. Temperatures were chosen near indoor values. Although all these experiments were performed between 20-30 °C, rapid moisture adsorbing capability of the material is expected to be enhanced at lower surrounding temperatures.

Surprisingly, the water-repellent property of the material remained intact even after adsorption of moisture from air. Corresponding AC, RC and CA over moisture adsorbed surfaces are presented in Figure 4b and Figure S18. This was further studied in detail with a moisture-saturated superhydrophobic surface where the saturation-adsorption of the coated surface was carried out through multiple adsorption cycles at 25 °C, presented in Figure 4c. CA over this moisture-saturated sample was 170° (Figure 4c, inset), similar to the untreated surface (Figure 1c). Non-wettability of the moisture-saturated surface was also studied in detail with DDT and VDAT (Figure 4d&e and Video V8). This can be correlated with the previously discussed

experiments in Figure 3e where even after long exposure to sunlight and normal laboratory conditions (it results in the moisture-saturated surface), surfaces retain their water-repelling characteristics. For better understanding of such moisture adsorption phenomenon over a functional superhydrophobic material, a molecular-surface-functionality model is presented in Figure 4f. While small AS molecules get wrapped over the clay particles through a spontaneous self-polymerization of secondary amines, OS molecules with hydrocarbon chain mostly stay perpendicular to the surface<sup>[15]</sup> and control the bulk non-wetting property of the surface by reducing the surface energy and by trapping air inside the assemblies. Although these assemblies restrict the penetration of water droplets, water vapor or moisture (blue dots) can easily diffuse between these giant molecular walls and get adsorbed with amine functionalities. Nitrogen atom-induced interaction between amine functionalities and water molecules is shown in Figure 4f, inset. In short, the local molecular structure (and dimension) with proper chemical functionalities impart this property to the new superhydrophobic material.

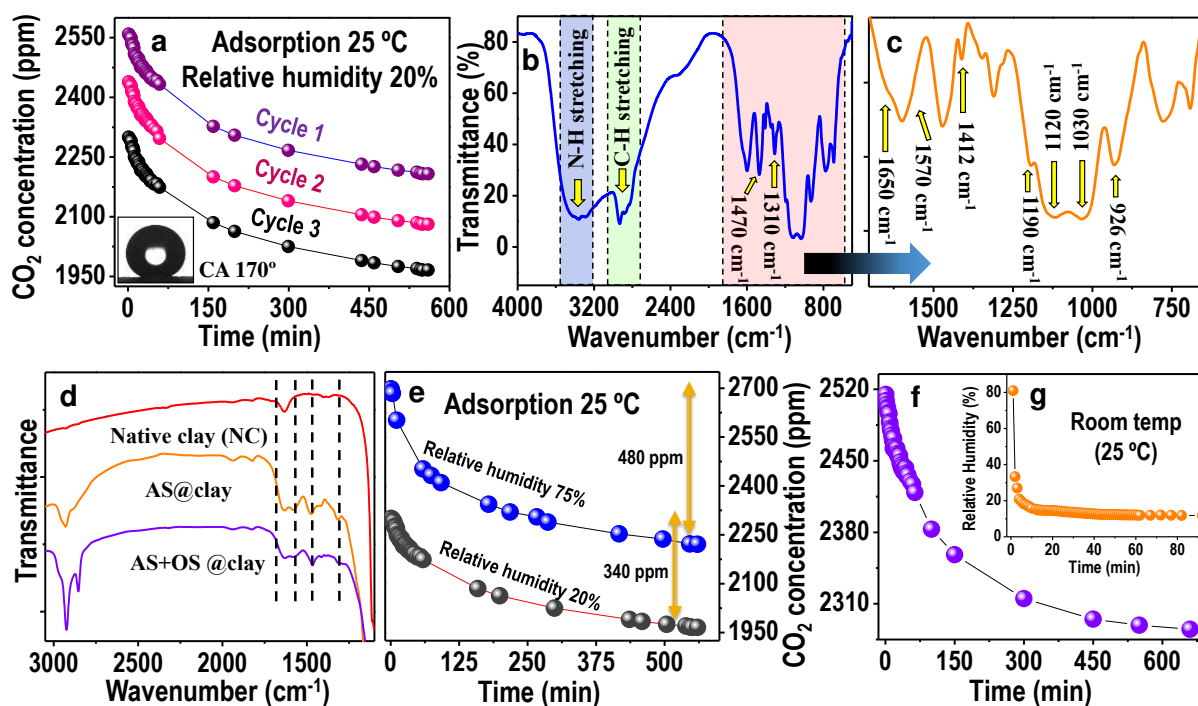


**Figure 5.** a, CO<sub>2</sub> capturing phenomenon over superhydrophobic surface at constant temperature.

Inset, static water contact angle over CO<sub>2</sub> adsorbed surface showing the retained

superhydrophobicity of the coated substrates. b, IR spectrum of only-amine (AS) after CO<sub>2</sub> adsorption. As clay has different IR active sites (in lower region), to locate the chemical changes properly upon CO<sub>2</sub> adsorption, only-amine was used here. Signatures correspond to the uptake of CO<sub>2</sub> are marked. c, Enlarged view of the area of interest in the spectrum b. d, IR spectra of CO<sub>2</sub>-adsorbed native clay, amine-clay and superhydrophobic clay. Characteristic features upon CO<sub>2</sub> adsorption are marked by dotted lines. These are present in both amine-clay and superhydrophobic clay but not observed in the IR spectrum of native clay. e, Influence of relative humidity on CO<sub>2</sub> adsorption process at constant temperature. f,g, Moisture and CO<sub>2</sub> adsorption performance (together) of the material at ambient conditions.

For CO<sub>2</sub> capturing experiments, the coated surface was subjected to an artificially-injected closed CO<sub>2</sub> environment. **Figure 5a** shows different cycles of CO<sub>2</sub> adsorption at 25 °C and a RH of 20%. Chemically, in this case also, molecular functionalities like primary and secondary amines facilitate the adsorption of CO<sub>2</sub>. This is schematically presented in Figure 4f where red color dots represent CO<sub>2</sub> molecules. Material shows an approximate CO<sub>2</sub> uptake of 480 ppm (10.90 mmol/L) under ambient conditions having 75% humidity. However, in this case, the adsorption kinetics was observed to be slower than the previous one (humidity adsorption). Unchanged wettability of the CO<sub>2</sub>-adsorbed material was measured with CA (Figure 5a, inset). To identify the nature of chemical-bonding between CO<sub>2</sub> molecules and amine groups, CO<sub>2</sub>-adsorbed material was characterized with IR spectroscopy (Figure 5b-d). As percentage of clay content is very high in the material and clay has various IR active modes in the lower region, only-amine (AS) which plays the key role to adsorb CO<sub>2</sub> was used to locate the chemical signatures related to the adsorption and interaction of CO<sub>2</sub> with amine groups (Figure 5b,c). Generally, CO<sub>2</sub> molecules bind with amine functionalities and form amide groups. Observed peak at 1650 cm<sup>-1</sup> relates to this C=O stretching of amides. Peaks at 1310 and 1412 cm<sup>-1</sup> correspond to the NCOO stretching which also confirms the binding of CO<sub>2</sub> with amine

functionalities. While peaks at 1030, 1120 and 1570  $\text{cm}^{-1}$  (shoulder) are associated with ammonium carbamate, peak at 1470  $\text{cm}^{-1}$  comes from  $\text{NH}_3^+/\text{NH}_2^+$ . Distinct peak at 926  $\text{cm}^{-1}$  relates to the N-H wagging of primary amine. However, these peaks are not present in pure-amine.<sup>[16]</sup> Figure 5d represents the IR spectra of  $\text{CO}_2$ -adsorbed NC, AS@clay and AS+OS@clay where none of the characteristic features of  $\text{CO}_2$  adsorption were seen for NC (features due to  $\text{CO}_2$  adsorption in AS@clay and AS+OS@clay are marked). Humidity being an influential parameter for chemical adsorption of  $\text{CO}_2$ , humidity dependent experiments were also performed at a constant temperature of 25 °C (Figure 5e). Adsorption of larger amount of  $\text{CO}_2$  in higher RH (75%) compared to the low humid condition (20% RH) again validate the  $\text{CO}_2$  capture mechanism of the material.<sup>[17]</sup> While at low RH (25%), surface was observed to show adsorption of  $350\pm 15$  ppm  $\text{CO}_2$ , at RH 75% it was in the range of  $480\pm 15$  ppm  $\text{CO}_2$  on an average. To demonstrate the real-life usability of the material, moisture and  $\text{CO}_2$  capture experiments were performed together at constant temperature (Figure 5f,g). As seen before, in this case also, rapid adsorption of water vapor/moisture was observed and it decreased below 20% RH within a few minutes. At the same time,  $\text{CO}_2$  capturing ability of the material remained unaltered. Having such important properties towards environmental issues along with its durable non-wettability, we believe that this multifunctional superhydrophobic material will enhance its usability in different technologies including paints, flexible electronics and microfluidic devices.

### 3. Conclusion

In conclusion, we demonstrate the development of a green and multifunctional waterborne superhydrophobic material having an enhanced environmental relevance. Ability to adsorb moisture and  $\text{CO}_2$  at the same time without affecting the water-repelling characteristics, makes this material novel and industrially valuable. Being synthesized in water and ambient conditions, it promotes bulk production and minimizes additional environmental concerns and safety



related issues. Durability of the coated surfaces against various external perturbations, revealed the applicability of the material in day-to-day life. This includes various paper-based technologies, clothing, packaging and many others. Molecular functionality-driven rapid adsorption of moisture at different temperatures, promotes the versatile use of the material for different purposes. CO<sub>2</sub> adsorption capability even in dry condition highlights the potential of the material as well. Finally, the ease of synthesis and eco-friendly nature of the material not only broadens its industrial adoptability, it also addresses the urgent environmental need towards reducing the impact of air pollution and climate change.

## 4. Experimental Section

### 4.1. *Materials*

All the chemicals were purchased from commercial sources and used without further purification. Kaolinite clay was purchased from Alpha minerals and chemicals (India). Octadecyltriethoxysilane (OS, 95%) was purchased from Gelest (USA). 3-(2-aminoethylamino)propyltrimethoxysilane (AS, commercial grade) was purchased from Rishichem Distributors (India). Ethanol, hexane, heptane, dimethyl sulfoxide (DMSO), and tetrahydrofuran (THF) were procured from RANKEM, India. All the chemicals were used without further purification. Sandpaper (P320) was purchased from a local hardware shop.

### 4.2. *Synthesis*

Chemical modification of the hydrophilic clay particles was performed solely in water through a wet chemical process (Figure 1a, S19). One pot synthesis of the material includes the mixing of two differently functionalized silane molecules, AS (1 ml) and OS (0.7 ml), with well-dispersed aqueous clay solution (2.75 wt%) at room temperature and was kept under vigorous stirring condition for 10-12 h. Although the silanes are generally very reactive in water, chemical attachment of OS with clay particles was controlled, as the solubility of OS in water

is very low because of the long hydrophobic tail. Having silane functionality in another end, this low surface energy molecule initially gets adsorbed on the hydroxylated surfaces of clay particles and slowly underwent hydrolysis forming chemical bond with the clay sheet. As-synthesized dispersed material was then spray coated over various substrates and kept for drying. Although the coated surfaces were dried at room temperature (32 °C) and showed excellent water-repelling characteristic, to enhance the evaporation rate of water, coated substrates were also allowed to dry in warm condition (50 °C) that does not change the chemical and physical properties of the material (Figure S20). Therefore, to prepare the bulk samples for multiple experiments, this condition (drying at 50 °C) was followed all the time.

#### 4.3. Long term stability of the material

Long-term stability of the material was tested through two different ways. In the first case, as synthesized material was immediately coated over the surfaces and kept for 3 months. In the second case, the synthesized material was stored for 3 months and then coated over the surfaces. In both the cases, surfaces showed similar water-repelling property compared to the freshly prepared samples (as-synthesized material immediately coated and dried). In addition, the stability of the chemical attachments of these molecules (AS and OS) with clay particles was also studied through IR spectroscopy. Here, the dried material was sonicated in water for 30 min and the supernatant was studied by IR spectroscopy (Figure S21). In the Figure, spectrum of the supernatant (blue) does not contain any characteristic peak of either AS (black) and OS (red). Whereas the spectrum was similar to pure water (orange).

#### 4.4. Droplet drag test (DDT) and vertical droplet adhesion test (VDAT)

For the drag test, a water droplet (~5  $\mu$ L) attached with a needle was dragged back and forth by 5 cm over a coated surface and the change was observed in the shape of droplet during the movement. Whereas in the second experiment, vertical droplet adhesion test, water droplet (~5  $\mu$ L) attached with a needle was moved up and down and pushed vertically over the surface to deform the shape of the droplet. Detachment of the water droplet from the superhydrophobic

surface without leaving any traces showed the extent of the water-repelling nature of the material. These were performed in different locations of the surface as well.

#### 4.5. *Sand paper abrasion and mechanical pressing test*

For sand paper abrasion test, sand paper was placed between the surface and a load of 50 g and moved for 5 cm back and forth. After each 10 consecutive cycles CA, AC and RC of water droplet over abraded surface were measured and presented in Figure 3a. This was continued for 100 cycles. For mechanical pressing test, coated superhydrophobic paper was subjected to a pressure of 264.4 atm (equivalent to the weight of 5 ton). In this case, after every 1 h, CA, AC and RC of water droplet was measured. This pressure treatment of 1 h corresponds to 10 complete cycles.

#### 4.6. *Oil-wash experiment*

For the oil-wash experiment, a coated filter paper was artificially wetted with viscous silicone oil. Being oleophilic in nature, oil adsorbs on the surface nicely and goes inside the rough surface structure. Adsorbed oil was then manually washed with ethanol and hexane. Washed filter paper was further kept inside hexane for 12 h and was tested with water after complete drying.

#### 4.7. *Chemical durability against organic solvents*

Durability of the coated surface against organic solvent was performed in two ways with THF, DMSO, ethanol, and heptane. Solvents were chosen having different polarity. In the first case, coated surfaces were washed with these solvents and tested with the movement of water droplets and self-cleaning property. For the second one, coated surfaces were immersed inside the organic solvents for 50 h in a closed container and tested with CA, AC, RC and CAH measurements every 5 h intervals.

#### 4.8. *Durability against environmental stresses*

Durability of the coated surface against various environmental stresses were evaluated by treating the surface with extreme temperature, direct sunlight and normal laboratory atmosphere

for long times. For temperature treatment, surfaces were kept at 150 °C and -80 °C for 2 h. Treated surfaces were tested with static and dynamic water contact angle measurements once they reached to ambient temperature. Change in wetting property of the surface upon exposure to sunlight and normal laboratory atmosphere for long time was tested by keeping the surfaces outside (under direct sunlight and laboratory environment) for 3 months. However, even after a year the surfaces were observed to retain their superhydrophobicity.

#### 4.9. *Temperature stability experiment*

For studying the stability of the material at higher temperature (>150 °C), the coated surfaces were tested at 200, 225 and 250 °C. In all the cases, to eliminate the aerial oxidation, surfaces were heated in vacuum condition for 30 mins. Non-wettability of the treated surfaces was examined with CA and VDAT. While till 250 °C, water droplets were observed to roll off nicely, above this, pinning of the droplets was seen.

#### 4.10. *Moisture and CO<sub>2</sub> adsorption experiments*

Both moisture and CO<sub>2</sub> adsorption experiments were carried out with coated filter paper in a closed container at constant temperature (25 °C). On an average approximately 1 g material was used to coat the filter papers. Reproducibility of such rapid moisture adsorption and CO<sub>2</sub> adsorption were studied with same coated filter paper for multiple time in a cyclic way. These are presented in Figure 4a & 5a. In between the experiments, coated surfaces were reactivated by desorbing the adsorbed water and CO<sub>2</sub> molecules at a relatively warm condition (50-60 °C) for 10 min.

### **Supporting Information**

Supporting Information is available from the Wiley Online Library or from the author.

### **Acknowledgements**

We thank the Department of Science and Technology, Government of India for constantly supporting our research program on nanomaterials. A.B. acknowledges support of INSPIRE Fellowship, Department of Science and Technology, Govt. of India. R.H.A.R. acknowledges support by European Research Council (ERC-2016-CoG No. 725513 “SuperRepel”) and the

Academy of Finland Centres of Excellence Programme (2014–2019). This work was supported by Finnish National Agency for Education. We thank Prof. Mahesh V Panchagnula for helping in bouncing of water droplets experiments.

Received: ((will be filled in by the editorial staff))

Revised: ((will be filled in by the editorial staff))

Published online: ((will be filled in by the editorial staff))

## References

- [1] a) T. Sun, L. Feng, X. Gao, L. Jiang, *Acc. Chem. Res.* **2005**, *38*, 644; b) G. Kwon, E. Post, A. Tuteja, *MRS Commun.* **2015**, *5*, 475; c) Y. Zheng, H. Bai, Z. Huang, X. Tian, F.-Q. Nie, Y. Zhao, J. Zhai, L. Jiang, *Nature* **2010**, *463*, 640; d) M. P. Sousa, J. F. Mano, *ACS Appl. Mater. Interfaces* **2013**, *5*, 3731.
- [2] a) K. Liu, M. Cao, A. Fujishima, L. Jiang, *Chem. Rev.* **2014**, *114*, 10044; b) H. Teisala, M. Tuominen, J. Kuusipalo, *Adv. Mater. Interfaces* **2014**, *1*, 1300026; c) S. Wang, K. Liu, X. Yao, L. Jiang, *Chem. Rev.* **2015**, *115*, 8230; d) G. B. Hwang, K. Page, A. Patir, S. P. Nair, E. Allan, I. P. Parkin, *ACS Nano* **2018**, *12*, 6050.
- [3] a) C. Peng, Z. Chen, M. K. Tiwari, *Nat. Mater.* **2018**, *17*, 355; b) J. E. Mates, T. M. Schutzius, I. S. Bayer, J. Qin, D. E. Waldrup, C. M. Megaridis, *Ind. Eng. Chem. Res.* **2014**, *53*, 222; c) D. Soto, A. Ugur, T. A. Farnham, K. K. Gleason, K. K. Varanasi, *Adv. Funct. Mater.* **2018**, *28*, 1707355.
- [4] a) Y. Lu, S. Sathasivam, J. Song, C. R. Crick, C. J. Carmalt, I. P. Parkin, *Science* **2015**, *347*, 1132; b) L. Li, B. Li, J. Dong, J. Zhang, *J. Mater. Chem. A* **2016**, *4*, 13677; c) X. Deng, L. Mammen, H.-J. Butt, D. Vollmer, *Science* **2012**, *335*, 67; d) X. Du, M. Wang, A. Welle, F. Behboodi-Sadabad, Y. Wang, P. A. Levkin, Z. Gu, *Adv. Funct. Mater.* **2018**, *28*, 1803765; e) D. Yoo, Y. Kim, M. Min, G. H. Ahn, D.-H. Lien, J. Jang, H. Jeong, Y. Song, S. Chung, A. Javey, T. Lee, *ACS Nano* **2018**, DOI: 10.1021/acsnano.8b05224; f) S. Pan, R. Guo, M. Björnalm, J. J. Richardson, L. Li, C.

- Peng, N. Bertleff-Zieschang, W. Xu, J. Jiang, F. Caruso, *Nat. Mater.* **2018**, DOI: 10.1038/s41563-018-0178-2.
- [5] a) K. Chen, S. Zhou, S. Yang, L. Wu, *Adv. Funct. Mater.* **2015**, *25*, 1035; b) T. Darmanin, F. Guittard, *Soft Matter* **2013**, *9*, 5982.
- [6] a) A. M. Rather, U. Manna, *ACS Appl. Mater. Interfaces* **2018**, *10*, 23451; b) Z.-h. Zhang, H.-j. Wang, Y.-h. Liang, X.-j. Li, L.-q. Ren, Z.-q. Cui, C. Luo, *Sci. Rep.* **2018**, *8*, 3869.
- [7] H. Ye, L. Zhu, W. Li, H. Liu, H. Chen, *ACS Appl. Mater. Interfaces* **2017**, *9*, 858.
- [8] a) A. Baidya, M. A. Ganayee, S. Jakka Ravindran, K. C. Tam, S. K. Das, R. H. A. Ras, T. Pradeep, *ACS Nano* **2017**, *11*, 11091; b) A. Baidya, S. K. Das, R. H. A. Ras, T. Pradeep, *Adv. Mater. Interfaces* **2018**, *5*, 1701523.
- [9] a) Y. Ren, Z. Lin, X. Mao, W. Tian, T. Voorhis, T. A. Hatton, *Adv. Funct. Mater.* **2018**, *28*, 1801466; b) R. Wang, J. Zhu, K. Meng, H. Wang, T. Deng, X. Gao, L. Jiang, *Adv. Funct. Mater.* **2018**, *28*, 1800634; c) V. Jokinen, E. Kankuri, S. Hoshian, S. Franssila, R. H. A. Ras, *Adv. Mater.* **2018**, *30*, 1705104.
- [10] a) Y. C. Jung, B. Bhushan, *ACS Nano* **2009**, *3*, 4155; b) L. Ye, J. Guan, Z. Li, J. Zhao, C. Ye, J. You, Y. Li, *Langmuir* **2017**, *33*, 1368; c) A. Das, J. Deka, A. M. Rather, B. K. Bhunia, P. P. Saikia, B. B. Mandal, K. Raidongia, U. Manna, *ACS Appl. Mater. Interfaces* **2017**, *9*, 42354; d) K. K. Jung, Y. Jung, C. J. Choi, J. S. Ko, *ACS Omega* **2018**, *3*, 12956.
- [11] L. Chen, X. Sheng, D. Wang, J. Liu, R. Sun, L. Jiang, X. Feng, *Adv. Funct. Mater.* **2018**, *28*, 1801483.
- [12] a) F. Geyer, C. Schönecker, H.-J. Butt, D. Vollmer, *Adv. Mater.* **2017**, *29*, 1603524; b) Y.-F. Lin, W.-W. Wang, C.-Y. Chang, *J. Mater. Chem. A* **2018**, *6*, 9489.
- [13] a) C. Serre, *Angew. Chem. Int. Ed.* **2012**, *51*, 6048; b) P. Z. Moghadam, J. F. Ivy, R. K. Arvapally, A. M. dos Santos, J. C. Pearson, L. Zhang, E. Tylianakis, P. Ghosh, I. W. H.

- Oswald, U. Kaipa, X. Wang, A. K. Wilson, R. Q. Snurr, M. A. Omary, *Chem. Sci.* **2017**, *8*, 3989.
- [14] T. Verho, C. Bower, P. Andrew, S. Franssila, O. Ikkala, R. H. A. Ras, *Adv. Mater.* **2011**, *23*, 673.
- [15] C. Nicosia, J. Huskens, *Mater. Horiz.* **2014**, *1*, 32.
- [16] S. Ek, E. I. Iiskola, L. Niinistö, *J. Phys. Chem. B* **2004**, *108*, 9650.
- [17] a) J. J. Lee, C.-H. Chen, D. Shimon, S. E. Hayes, C. Sievers, C. W. Jones, *J. Phys. Chem. C* **2017**, *121*, 23480; b) A. Gholidoust, J. D. Atkinson, Z. Hashisho, *Energy & Fuels* **2017**, *31*, 1756.

A waterborne, fluorine-free, robust superhydrophobic material has been developed from hydrophilic clay particles that captures moisture and CO<sub>2</sub> simultaneously. Chemically, adsorption of moisture and CO<sub>2</sub> need polar surfaces and superhydrophobicity/water-repellency requires apolar/non-polar surfaces. Both of these properties are controlled here by molecular functionalities of different dimensions.

**Keywords** Superhydrophobicity, environment-friendly, waterborne, robust, moisture sorption and CO<sub>2</sub> capture

Avijit Baidya<sup>a,b,c</sup>, Anagha Yatheendran<sup>a</sup>, Tripti Ahuja<sup>a</sup>, Chennu Sudhakar<sup>a</sup>, Sarit Kumar Das<sup>c</sup>, Robin H.A. Ras<sup>b,d</sup>, Thalappil Pradeep<sup>a,\*</sup>

### Waterborne Fluorine-Free Superhydrophobic Surfaces Exhibiting Simultaneous CO<sub>2</sub> and Humidity Sorption

ToC figure

